DEPARTMENT OF METEOROLOGY
THE UNIVERSITY OF WISCONSIN
MADISON, WISCONSIN

AN ANALYSIS OF DIURNAL VARIATIONS IN TIROS II RADIATION DATA

ELFORD G. ASTLING
LYLE H. HORN

THE ROLE OF SYNOPTIC SCALE VARIATIONS OF INFRARED RADIATION IN THE GENERATION OF AVAILABLE POTENTIAL ENERGY

JAMES L. CORCORAN
LYLE H. HORN

ANNUAL REPORT

THE RESEARCH REPORTED IN THIS DOCUMENT
HAS BEEN SUPPORTED BY
THE UNITED STATES WEATHER BUREAU
GRANT WBG-10, PROJECT 4

OCTOBER, 1964

DEPARTMENT OF METEOROLOGY
THE UNIVERSITY OF WISCONSIN
MADISON, WISCONSIN

AN ANALYSIS OF DIURNAL VARIATIONS IN TIROS II RADIATION DATA

ELFORD G. ASTLING
LYLE H. HORN

THE ROLE OF SYNOPTIC SCALE VARIATIONS OF INFRARED RADIATION IN THE GENERATION OF AVAILABLE POTENTIAL ENERGY

JAMES L. CORCORAN
LYLE H. HORN

ANNUAL REPORT

THE RESEARCH REPORTED IN THIS DOCUMENT
HAS BEEN SUPPORTED BY
THE UNITED STATES WEATHER BUREAU
GRANT WBG-10, PROJECT 4

OCTOBER, 1964

An Analysis of Diurnal Variations in TIROS II Radiation Data

Elford G. Astling and Lyle H. Horn

Abstract

Twenty-six days of TIROS II data are used to study diurnal variations of infrared radiation (7-32 microns). A diurnal trend is noted. When the data are partitioned into land and ocean data, diurnal variations are found in both cases. A diurnal trend in the land cases was expected; however, the trend over oceanic areas was not anticipated. An analysis of sampling procedures used in the study indicates that the oceanic trend is not the result of a sampling bias. The possible causes for this trend include a number of instrument calibration problems and a number of physical processes occurring within the earth-atmosphere system. Because a number of possible causes exists, the authors suggest that dirunal variations in TIROS II infrared observations be interpreted with caution.

1. Introduction

Satellite observations of infrared radiation are providing the meteorologist with the first direct measurements on a global scale of the differential cooling processes which are a basic source of atmospheric circulation. Because the satellite is a relatively new instrument, many of the initial studies which employ satellite data are concerned either with the gross features described by the data or with attempts to properly interpret the data. In an earlier study, the authors(Astling and Horn, 1964) used TIROS II measurements to obtain separate latitudinal profiles of infrared radiation (7-32 microns) for continental and oceanic areas. The distinct difference in the land and ocean profiles which were revealed could be reasonably interpreted in terms of distribution of cloudiness and surface temperature distribution over land and ocean areas. The question then arose as to whether day-night differences between oceanic and land areas might likewise be apparent. Consequently, the same data were used in an attempt to describe the diurnal variations of infrared radiation for continental and oceanic regions.

A presence of diurnal variations of infrared radiation in the 7-32 micron band has a number of implications. Through a careful analysis of <u>specific</u> synoptic cases over land areas, Fritz (1963) has shown that the "window" channel of the scanning radiometer aboard TIROS II can readily detect diurnal

differences in the earth's surface temperature in clear areas. Therefore, the existence of a diurnal trend in a large sample of infrared measurements (7-32 microns) made over land areas can best be explained as resulting from the contribution of day-night differences in radiation emitted from the surface and passing through the atmospheric "window." However, the appearance of a diurnal trend in a large sample of oceanic cases is less easily explained. Since it is generally agreed that the surface of the ocean experiences only very small diurnal temperature changes, one should expect little or no diurnal variation in the infrared emission from the ocean surface.

In this study the TIROS II channel 4 data have been partitioned according to the local hour of the observation, and the diurnal variations of infrared radiation have been analyzed for both land and ocean areas. Because of the possibility of a sampling bias, the data have been further broken into subsamples and the diurnal trends analyzed within each subsample.

2. Data And Procedures

The data used in this analysis were read from daily composite radiation maps of the infrared radiative flux in the 7 to 32 micron band as measured by the scanning radiometer aboard TIROS II. With proper corrections for the spectral

characteristics of the radiometer, these measurements represent the total long-wave radiation emitted from the earth-atmosphere system. The period of study consisted of 26 selected days between November 26, 1960, and January 6, 1961, for which composite radiation maps were prepared by the Meteorological Satellite Laboratory of the United States Weather Bureau. The data were read along individual subsatellite tracks at 5 degree intervals of longitude between latitudes 50°N and 50°S. Cases from overlapping orbits were not used because in the preparation of the composite maps these observations were averaged without regard to the time of observation. Consequently, the data used here tend to be weighted toward observations made between latitudes 30°N and 30°S. By using only subsatellite observations the sample was limited to observations made at nadir angles of less than 26°, and thus limb darkening effects are very small (Wark et al, 1961). For a more complete discussion of the data sample used here the reader is referred to Astling and Horn (1964).

To investigate diurnal variations of the long-wave radiation measurements, the data for the 26 days were partitioned according to the local hour of observation. However, because of the possibility of a sampling bias, a simple description of the diurnal variations was not possible. Due to the time of launch of TIROS II and the limited number of days with open mode observations, 18 of the 26 days were from periods when the

satellite was over the Southern Hemisphere (summer) during the day and over the Northern Hemisphere (winter) at night. This would weight daytime averages toward higher values and nighttime averages toward lower values. In addition, there was an apparent degradation of the channel 4 sensors during the 26 days. The daily mean for the entire radiation map decreased from 0.36 ly min^{-1} during the first few days after launch to 0.31 ly min^{-1} six weeks later. Consequently, if more of the daytime observations were made during the early part of the period and more of the nighttime observations during the later part, a tendency toward a diurnal trend could result. In an attempt to reduce the effect of these sampling biases, a statistic which includes both deviations from latitudinal means and deviations from daily means was employed. The formation of the statistic is briefly described below.

Let F_n represent a single infrared observation taken at hour i at latitude j on day t. Using the above notation the mean deviation of the infrared flux for local hour i is

$$\overline{\Delta F_i} = \frac{1}{2N_i} \sum_{n=1}^{N_i} \left[(F_n - \overline{F_j}) + (F_n - \overline{F_t}) \right]$$

where $\overline{F}_j$ is the 26 day mean for latitude j, $\overline{F}_t$ is the mean radiation for the entire map on day t, and N_i is the total number of observations for the i^{th} hour. The advantage of a statistic such as this is that it compensates for some of the

latitudinal and temporal bias in sampling and at the same time combines the entire data sample into one statistic. However, to further reduce the effects of sampling bias, the data were subsequently partitioned into smaller time intervals (i.e., groups of days) and also into separate hemispheres.

3. Discussion of Results

The departures of the hourly means which are obtained when the above statistic is applied to the entire data sample are presented in Figure 1. Positive deviations exceeding $+0.02$ ly min^{-1} are noted during the middle of the day while nighttime deviations are, for the most part, negative. Since the data presented by this figure include both land and ocean cases, this diurnal trend was expected.

To further investigate the significance of diurnal variations, the data were partitioned into land and ocean cases and the statistic computed for each. The results are shown in Figures 2 and 3. Satellite data from near coastlines were not included; consequently, the total number of cases shown in Figures 2 and 3 do not equal those presented in Figure 1. It should also be noted that the deviations presented in all the figures of this study involve deviations from the subsatellite latitudinal means obtained by Astling and Horn (1964). Consequently, the deviations do not add to zero. Since we are interested only in the diurnal variations, this

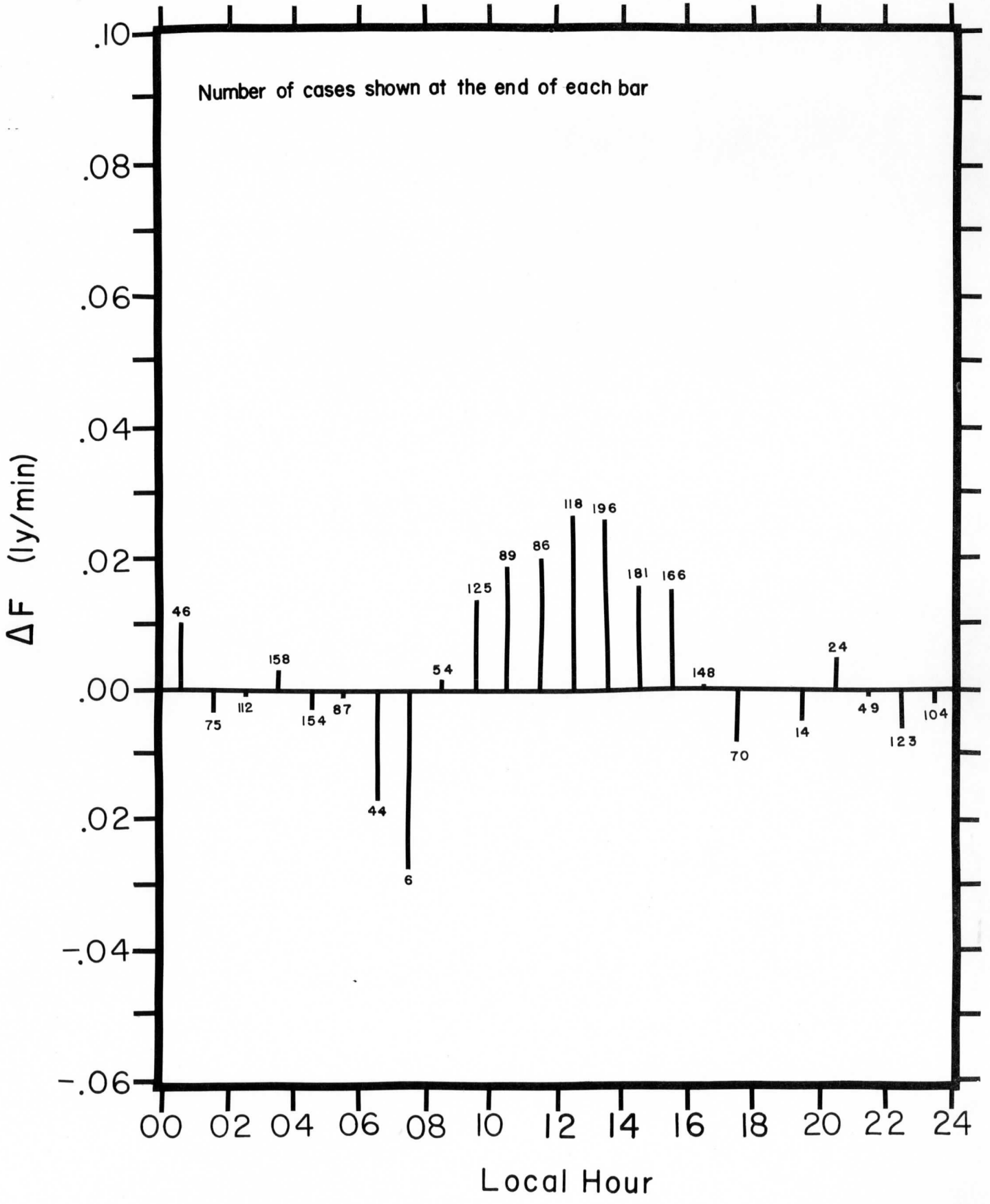

Figure 1 (All Cases)

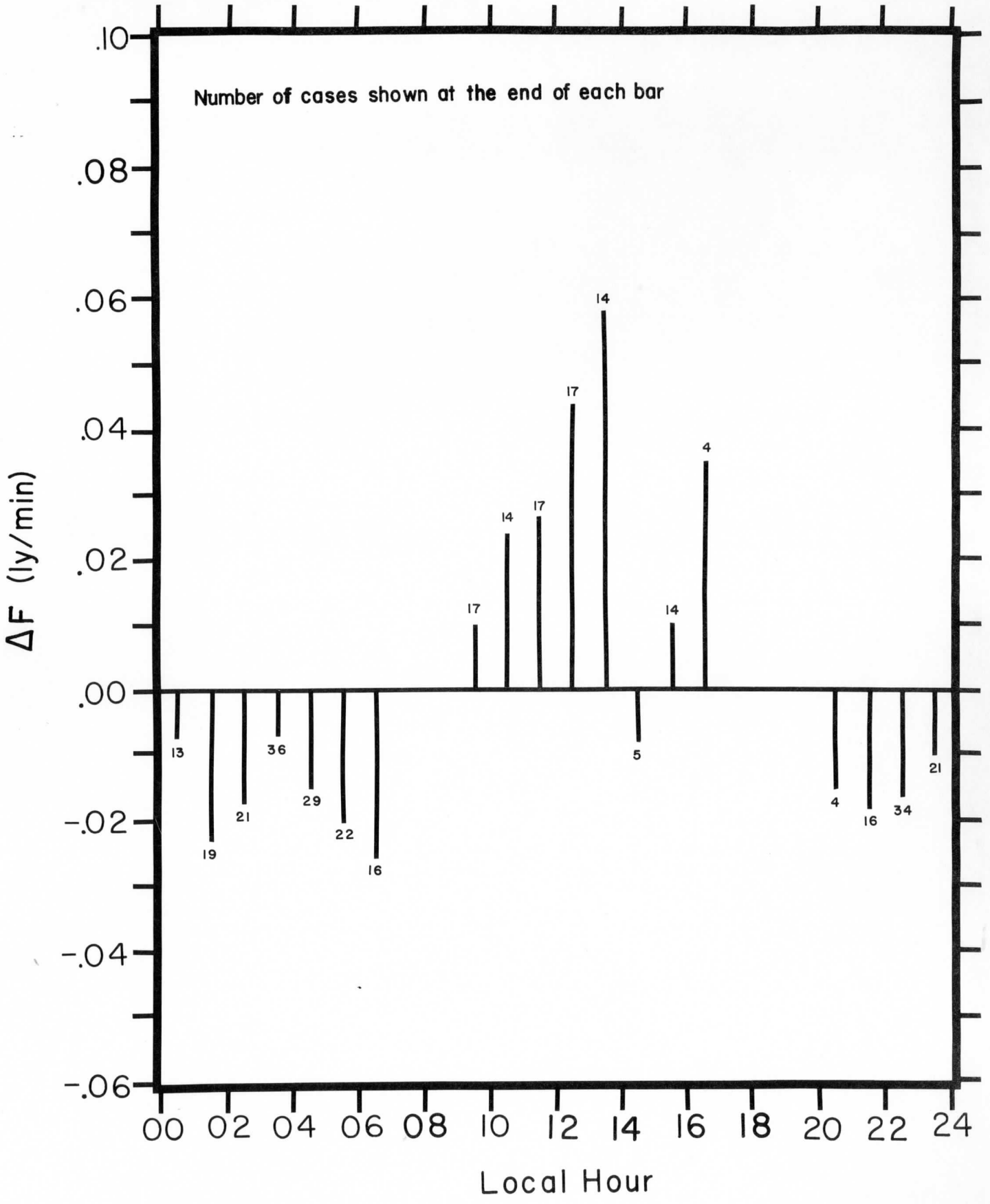

Figure 2 (Land Cases)

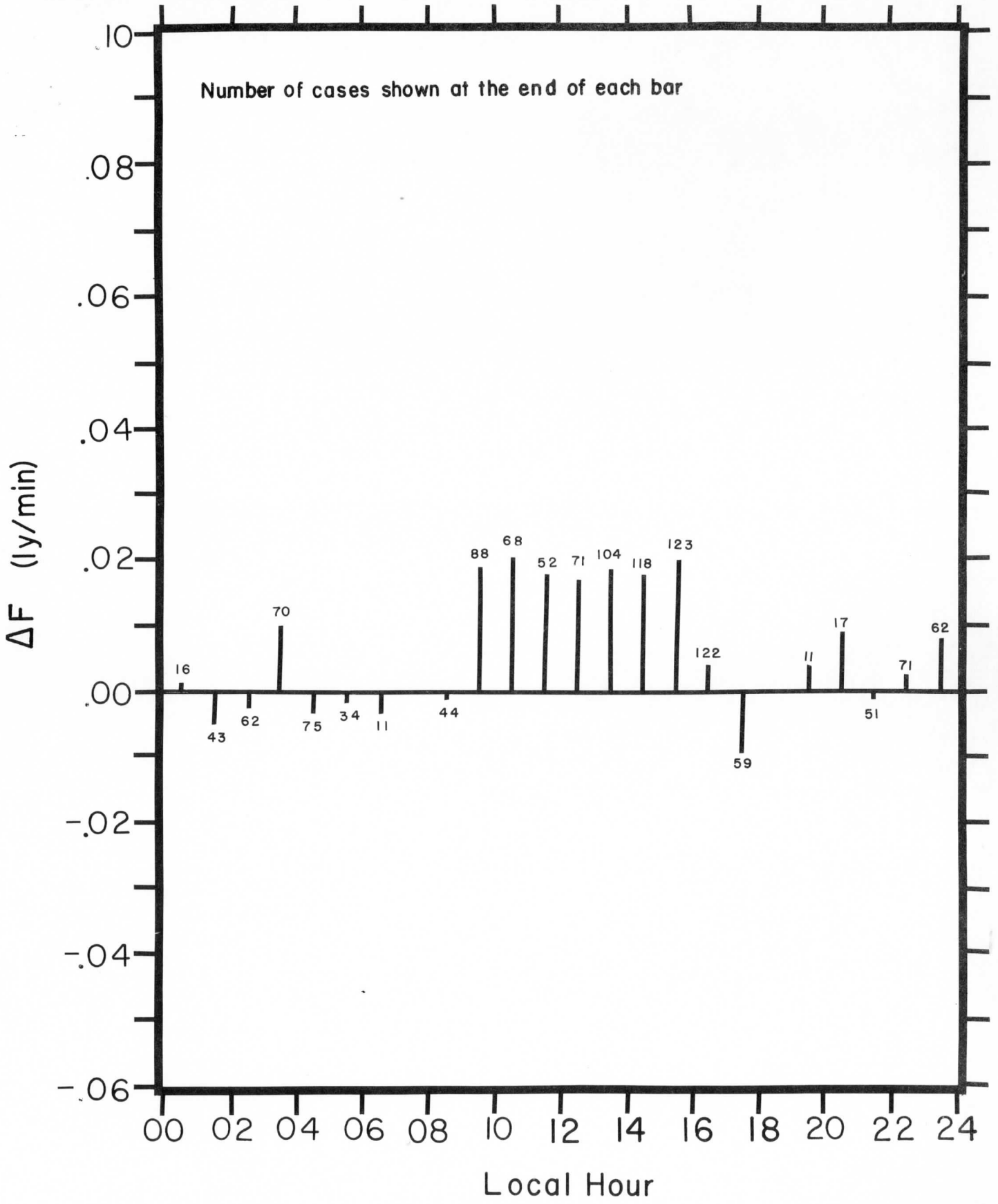

Figure 3 (Ocean Cases)

is of no consequence. As expected, the land cases (Figure 2) show a definite diurnal trend with deviations in excess of +0.04 ly min^{-1} during midday and about -0.02 ly min^{-1} during the late nighttime hours. Although any number of factors could produce a diurnal variation over land areas, the most reasonable explanation is a diurnal variation of infrared radiation leaving the earth's surface and passing through the atmospheric window.

The diurnal variation for the ocean cases which is presented in Figure 3 was not expected. The positive daytime deviations, averaging about +0.02 ly min^{-1} between 0900 and 1500 local time, stand out. Because of the very small diurnal temperature variation at the sea surface, these variations cannot be as easily interpreted as the land cases variation. Although it is not the intent of this paper to establish the reason for these oceanic variations, a number of possibilities will be noted. They may be classified as: a) data sampling problems, b) instrument calibration problems, and/or c) physical processes occurring within the earth-atmosphere system.

a) Data Sampling Problems

The ideal method of testing for diurnal trends in oceanic data is to study the infrared flux variations over a small, fixed area of the oceans. Unfortunately, an adequate sample of TIROS II data for such a limited area study does not exist

The authors attempted such a local study but could draw no conclusions because of insufficient data. Thus, to obtain any results, an approach which employed the entire data sample was required. Since the use of a large amount of data introduces sampling problems, a statistic which tends to compress observations taken on a global scale over a period of 42 days to relatively local observations was needed. The statistic used here tends to accomplish this. By employing deviations from the 26 day latitudinal means, the statistic removes some of the seasonal (Northern Hemisphere winter, Southern Hemisphere summer) variations from the data. Likewise, the use of deviations from daily means reduces sampling problems which could arise from the apparent degradation of the sensors. By combining the deviations it was possible to obtain a significantly large data sample. Because of the nature of the statistic and the size of the data sample, the diurnal trend which appears in Figure 3 is very likely real.

However, to further test the validity of the trend, the authors partitioned the data into subsamples and studied each separately. The first partitioning consisted of dividing the data into Southern and Northern Hemisphere land and ocean cases. This division reduces problems arising from the tendency of the satellite to observe one hemisphere at night and the other during the day. The results of this partitioning are presented

in Figures 4-7. Since it is based on the largest of the four subsamples, Figure 4 (Southern Hemisphere ocean cases) is statistically the most significant. It shows diurnal differences with appreciable positive deviations occurring between 0900 and 1500 local time. The Northern Hemisphere ocean data (Figure 5) show predominantly positive values, but the daytime values tend to be largest. As expected, both the Southern and Northern Hemisphere land cases (Figures 6 and 7) show definite diurnal variations.

The data were also partitioned according to the number of days after launch (DAL). This partitioning permits an analysis of the data within periods during which any degradation of the sensors is relatively small. In this partitioning, no attempt was made to study land-ocean differences. Because six groups of days were used, the data samples for each group were relatively small. Thus, rather than presenting the mean deviation for each hour, the hours were combined into daytime observations (0700-1800 local time) and nighttime observations (0100-0600 and 1900-2400 local time). The results are presented in Figure 8. In five out of the six periods, the daytime mean deviations are definitely larger than the nighttime values, indicating that the diurnal effect is relatively independent of the period of sampling. In the second sample (DAL 19, 20, 21) the nighttime values are only slightly greater. The results shown in Figure 8 combined with those already noted in Figures

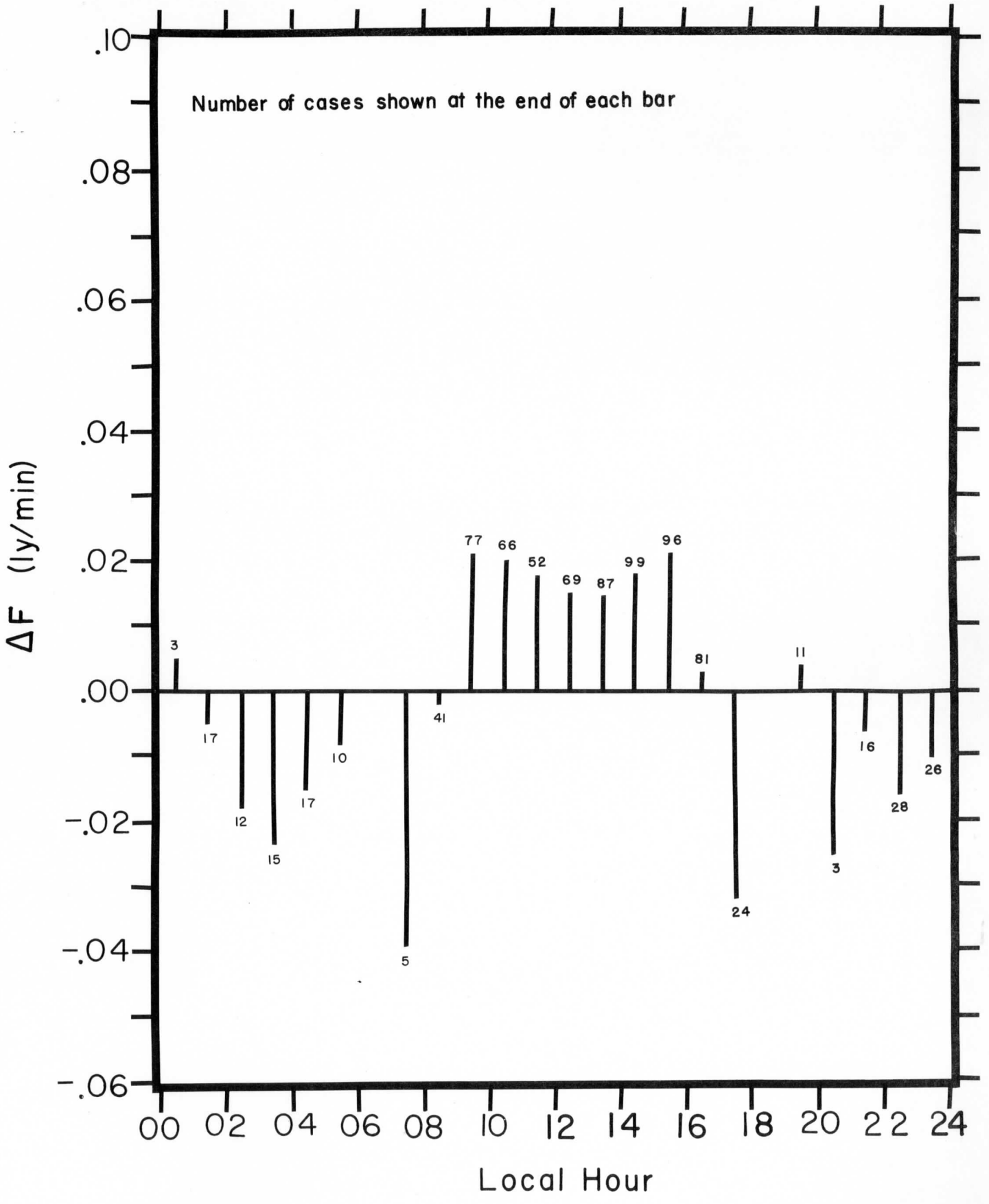

Figure 4 (Southern Hemisphere Ocean Cases)

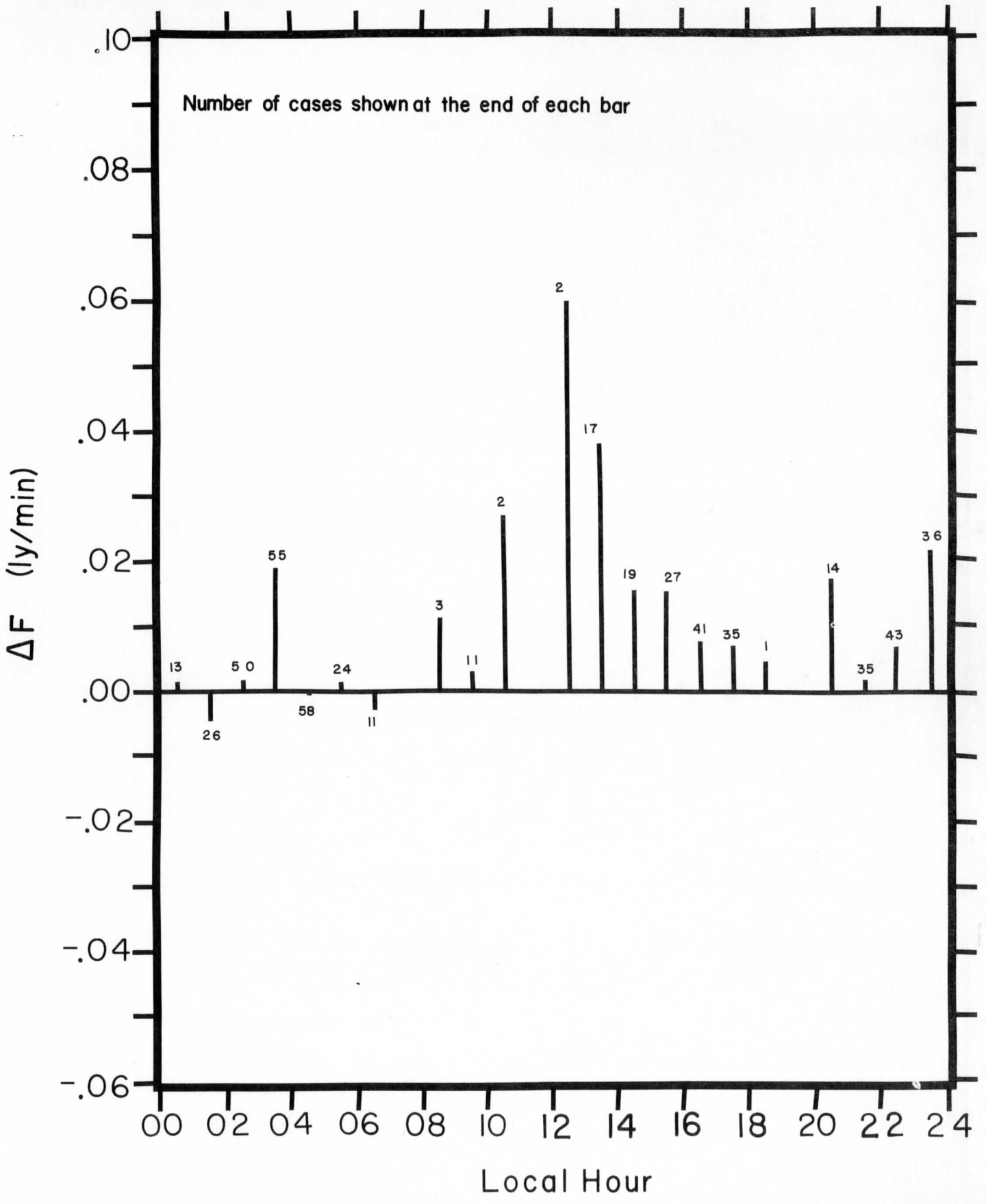

Figure 5 (Northern Hemisphere Ocean Cases)

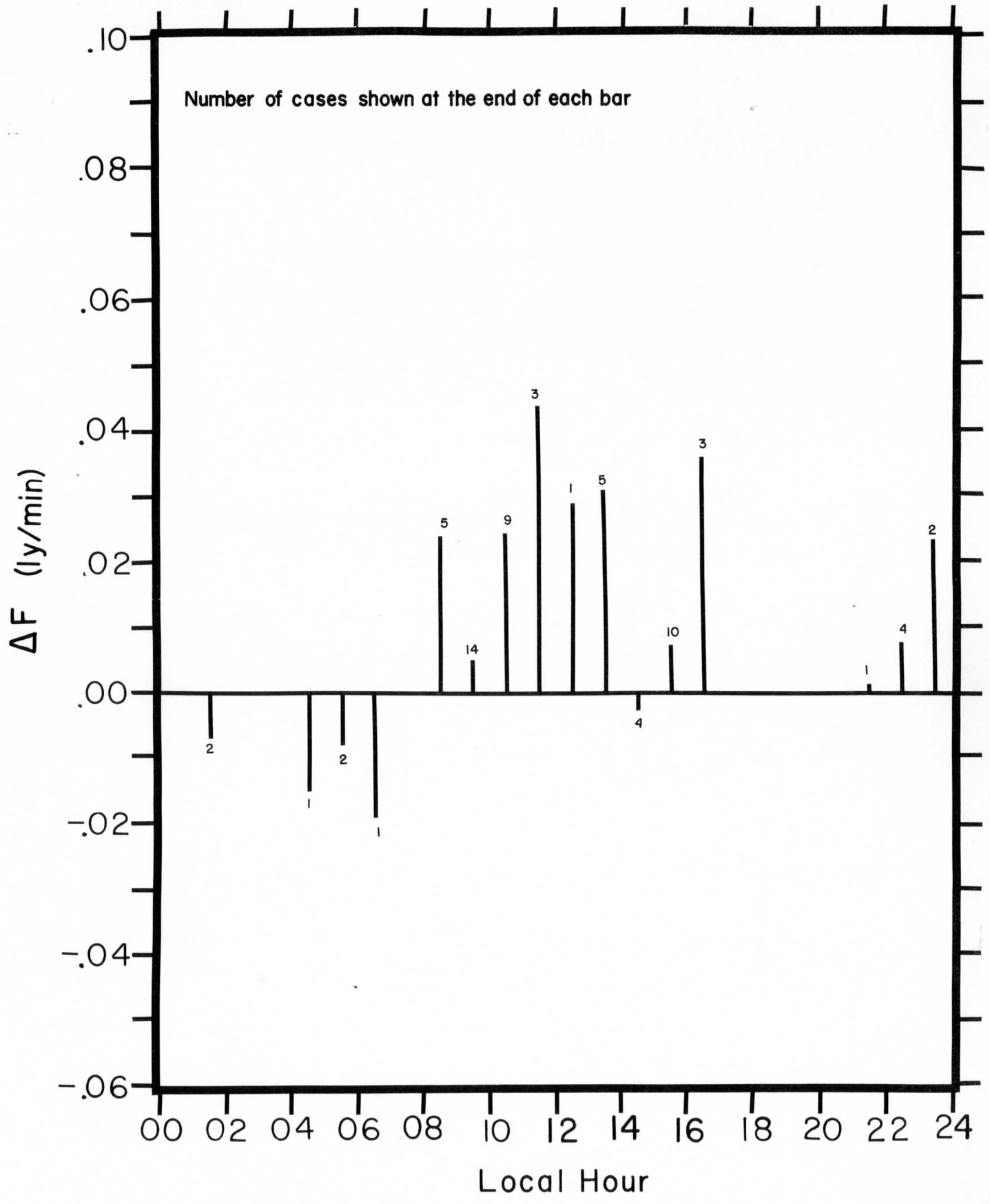

Figure 6 (Southern Hemisphere Land Cases)

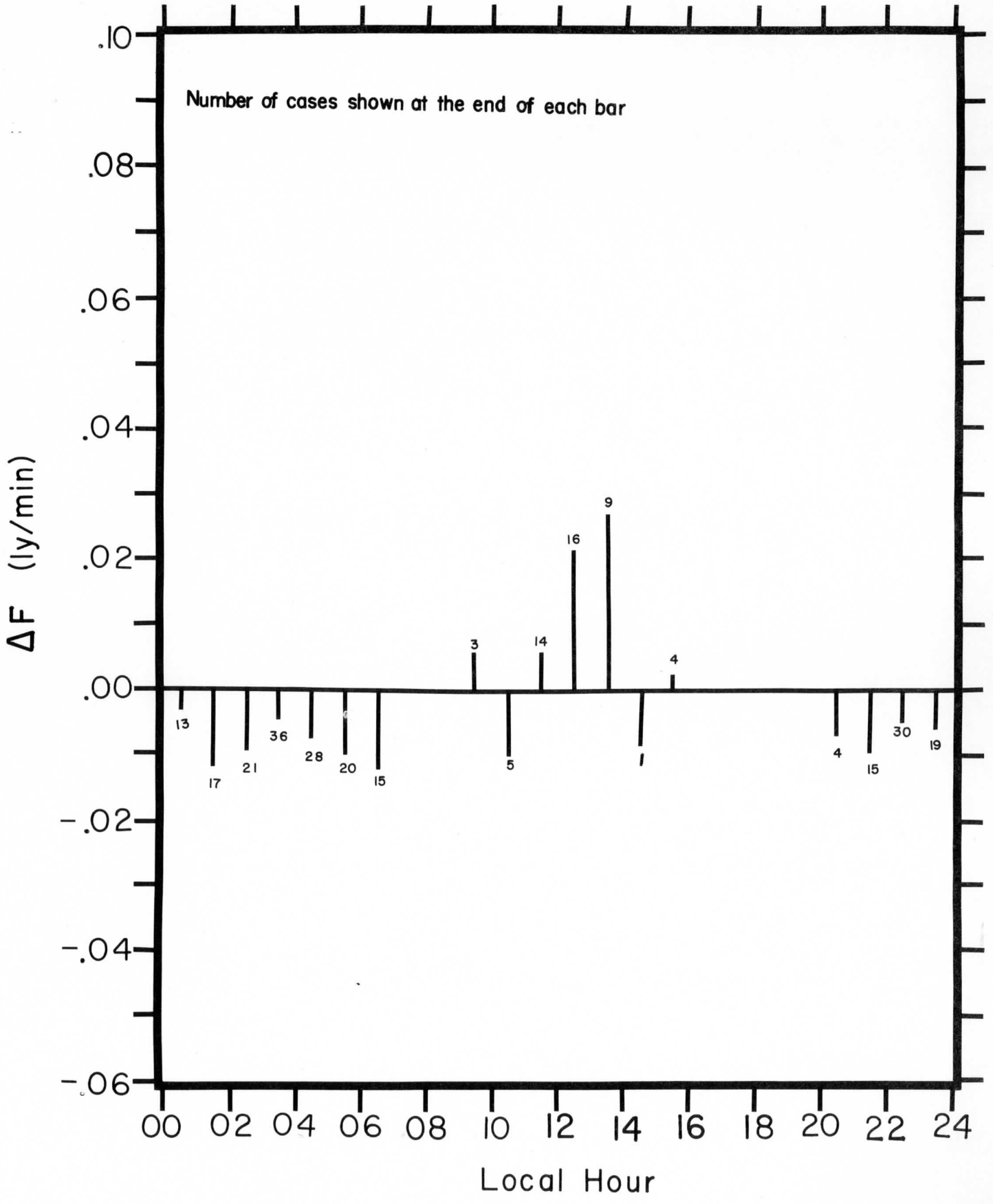

Figure 7 (Northern Hemisphere Land Cases)

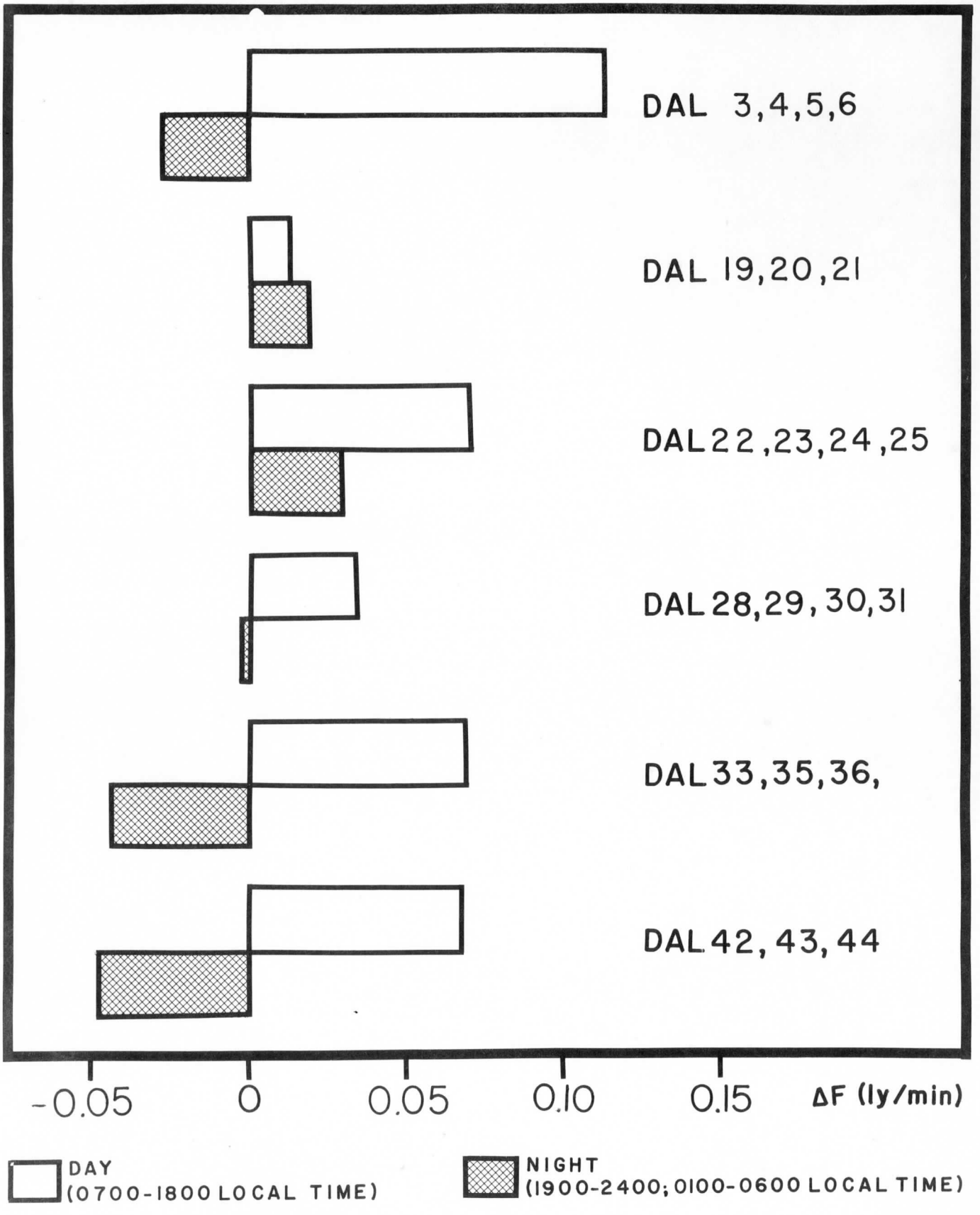

Figure 8 Partitioning of Data according to Days After Launch

1-7 present a rather convincing argument as to the existence of diurnal variations in the TIROS II Channel 4 data.

b. Instrument Calibration Problems

It is very possible that the diurnal variations are the result of calibration problems for the TIROS II satellite. The fact that the daytime observations over the oceans are significantly higher than nighttime observations suggests that direct heating of the satellite by the sun may be responsible. According to the TIROS II Radiation Data User's Manual (1961), the Channel 4 radiometer is affected by the radiometer housing and package temperatures. To correct for this effect, the mean temperature for each orbit was used rather than the actual temperatures of the housing and package at the time of observation. The difference between the mean temperature for the orbit and that at the time of a single observation varies within $\pm$ 3° C. Thus, during a single orbit there may be a variation in the amount of heat transferred (either by conduction or radiation) from the housing and package to the sensors. Such a variation may be sufficient to produce the diurnal differences noted in Figure 3. However, this argument for direct heating is somewhat weakened by the occurrence of uniformly high values from 0900 to 1500 local time. If direct heating were responsible, one might expect the highest values to occur at about the time the satellite leaves the sun. It is also possible that direct heating of the electronic compo-

nents of the satellite may be sufficient to influence the raw observation telemetered to earth. Because of the complexity of these heating effects, it is beyond the scope of this paper to firmly establish their effect in causing diurnal variations.

Bandeen (1964) has suggested another possible instrumental cause for the variations. He has noted a lack of balance between the wall and floor sensors aboard TIROS II. Because of the satellite orientation, there is a tendency for one sensor to observe the night portions of the earth and the other the day portions. This inbalance could cause the variations noted here.

It is also possible that the infrared sensors may absorb small amounts of reflected solar radiation. If any solar radiation reflected from cloud tops or the earth's surface reaches the sensor, the daytime maxima noted in this study could result.

In general, it seems that instrument problems such as direct heating or unbalanced sensors contribute to systematic variations in the data. However, whether these effects are the cause of the diurnal variations found in this particular data sample remains an unsolved problem.

c. Physical Processes Occurring Within the Earth-Atmosphere System

If the diurnal trends noted in the oceanic data are not the result of sampling bias or instrumental calibration, they

must result from some diurnal physical process occurring within the atmosphere or at the ocean surface. One possibility is that there is a diurnal variation in the upward emission of long wave radiation from the three principal radiative gases in the atmosphere - ozone, carbon dioxide, and water vapor. Kuhn (1963) estimates that the radiative contribution of ozone to the infrared flux is only 0.003 ly min^{-1}. Obviously, diurnal variations due to ozone emission are negligible. Carbon dioxide emission, which amounts to about 17 per cent of the total outward flux, is primarily a function of the temperature of the entire depth of the atmosphere, and thus it should have no significant diurnal variation. Since the water vapor content of the atmosphere over the oceans is generally thought to be quite constant from day to night, there appears little reason to expect that it is a contributing factor in producing the diurnal variations of infrared flux. Therefore, the diurnal effects of the radiative gases are not important.

The existence of a diurnal variation of clouds over the ocean could cause day-night differences in infrared flux. If there is more cloudiness - especially middle and high cloudiness - during the night than during the day, the type of diurnal trend shown in Figure 3 could be expected. Bryson (1951) has found a small diurnal variation of cloudiness and rainfall frequency with maximum occurrences at night. Kraus (1963), in a harmonic analysis of daily variation of rainfall at

several oceanic stations, also found some evidence of a diurnal variation of cloudiness over oceans during the summer. More recently, Rasool (1964) combined "window" channel data from TIROS III with cloud data obtained by Arking (1964) and surface climatological data in an attempt to describe the nighttime latitudinal distribution of cloudiness. His results led him to conclude that over the Southern Hemisphere, which is largely oceanic, the percentage of cloudiness at night is much greater than during the day. Over the Northern Hemisphere he found the reverse, less cloudiness at night than during the day. Although the Southern Hemisphere oceanic graph (Figure 4) presents a diurnal trend of infrared radiation which could be interpreted as supporting Rasool's Southern Hemisphere findings, the Northern Hemisphere data used in this study contradict his results. Consequently, it is impossible to make a meaningful comparison between the results of the two studies. However, the many possible causes for diurnal variation mentioned here indicate that the cloudiness explanation should be used with caution.

A diurnal variation in the height of cloud tops could produce diurnal infrared radiation variations as effectively as variations in cloud amounts. Nocturnal cooling at the top of the clouds can produce instability and further vertical development of the clouds. Thus the nighttime flux of radiation from the cloud tops would occur from higher levels and at

lower temperatures. It is also possible that absorption of solar radiation by clouds could play a role in producing day-night differences in the long-wave radiation emitted from cloud tops. Robinson (1958), and Korb and Moller (1962) have estimated that solar absorption by clouds of large vertical extent may equal or exceed 0.20 ly min^{-1}. This absorption may warm the cloud tops sufficiently to produce a greater outward flux of radiation during the day than during the night. However, before such possibilities as variations in the heights of cloud tops or diurnal heating of clouds at a fixed height can be seriously regarded, improved quantitative measurements of these effects must be made.

Finally, one remaining possibility - although remote - should be mentioned. It is possible that there is a diurnal variation of temperature at the very surface of the sea. Most studies of sea surface temperatures measure the temperature at some small distance below the surface. Thus the "skin" of the sea surface may actually possess a somewhat different temperature from that normally attributed to the surface of the sea. If it does, it is possible that it experiences diurnal variations, and thus produces day-night variations in the radiation emitted from the sea surface. However, because of the mixing generally associated with the surface water of the oceans, it seems unlikely that such diurnal differences could be large enough to affect the satellite measurements.

The possible physical causes for diurnal variations of infrared radiation are indeed numerous. An adequate evaluation of them would require a number of rather difficult studies. As more satellite data become available, such studies will be necessary.

4. Summary and Conclusions

The TIROS II Channel 4 data used in this study show a diurnal trend in the infrared radiation emission from the earth-atmosphere system. Although the diurnal variation over land areas was expected, the variation over oceanic areas was not. The oceanic diurnal variations may be produced by either biases in data sampling, instrument calibration problems, physical processes occurring with the earth-atmosphere system, or a combination of these. Since a statistic designed to reduce any sampling bias was used, and because the diurnal effect also appears in subsamples of the data, it is likely that the diurnal trend is not the result of sampling problems.

Direct heating of the satellite package by the sun may result in a transfer of heat to the sensor or may affect the electronic components in such a way as to produce the diurnal variations. The existence of an inbalance between the wall and floor sensors of TIROS II may also be the cause. Because of the complexity of these instrumental difficulties, it is beyond the scope of this paper to attempt a detailed description of

their effect on the data.

Any of a number of physical processes could also produce day-night variations in infrared flux over the ocean. Diurnal variations in cloudiness (or the height of the cloud tops) provide an appealing explanation of the radiation variations. However, before the cloudiness explanation (or any other physical explanation) is given as the cause of the diurnal variations, considerable attention should be given to the possibility that they are produced by the instrument calibration difficulties mentioned above.

The results of this study suggest that at the present stage of satellite meteorology considerable caution should be taken in interpreting day-night differences of infrared radiation which appear in large samples of data. It seems that as more satellite data become available, increased studies of the diurnal differences on a local scale should be undertaken. Such relatively "controlled" studies should aid in developing a proper interpretation of the data.

5. Acknowledgements

The authors wish to thank Mr. Donald Johnson, Major James Corcoran, and Mr. William Smith for their assistance in the study and Professor Verner Suomi for his comments concerning the possibility of satellite calibration difficulties. This study has been supported by United States Weather Bureau Grant No. 10, Project 4.

References

Arking, A., 1963: The Latitudinal Distribution of Cloud Cover from TIROS III Photographs. Institute of Space Studies, NASA.

Astling, E. G., and L. H. Horn, 1964: Some Geographical Variations of Terrestrial Radiation Measured by TIROS II. Journal of the Atmospheric Sciences, Vol. 21, 30-34.

Bandeen (1964) Personal communication.

Bryson, R. A., 1951: Studies on the Weather of the Tropical West Pacific by Means of the Cloudform Stability Scale. Bulletin of the American Meteorological Society, Vol. 32, 174-182.

Fritz, S., 1962: The Diurnal Variation of Ground Temperature as measured from TIROS II. Journal of Applied Meteorology, Vol. 2, 645-648.

Korb, Gunther, and Fritz Möller, 1962: Theoretical Investigation on Energy Gain by Absorption of Solar Radiation in Clouds. Institute, München, Germany, Final Technical Report, Contract DA-91-591-EUC-1612.

Kraus, E. B., 1963: The Diurnal Precipitation Change over the Sea. Journal of the Atmospheric Sciences, Vol. 20, 551-556.

Kuhn, P. M., 1963: Soundings of Observed and Computed Infrared Flux. Journal of Geophysical Research, Vol. 68, 1415-1420.

Robinson, G. D., 1958: Observations from Aircraft of Surface Albedo and the Albedo and Absorption of Clouds. Archiv für Meteorologie Geophysik und Biolimatologie, B9, 28-41.

Staff Members, 1961: TIROS II Radiation Data User's Manual. Greenbelt, Md., Goddard Space Flight Center.

Wark, D. Q., G. Yamamoto and J. H. Lienesch, 1962: Methods of Estimating Infrared Flux and Surface Temperature from Meteorological Satellites. Journal of the Atmospheric Sciences, Vol. 19, 369-384.

Wexler, R., 1963: Synoptic Interpretations and Heat Balance Determination from TIROS II Radiation Data. Scientific Report No. 1, Contract No. A19 (628)-429, Aracon Laboratories, Concord, Mass. 22 pp.

The Role of Synoptic Scale Variations of Infrared Radiation in the Generation of Available Potential Energy

James L. Corcoran and Lyle H. Horn

Abstract

Satellite radiation data are used to investigate the role of infrared radiation in the generation of eddy available potential energy. A significant difference in the outgoing radiation above surface cyclones and anticyclones is noted. The generation associated with 500 mb waves is estimated by computing the covariance of infrared radiation and the 1000-500 mb thickness, and a small positive generation is noted. A study of the generation as a function of scale size reveals that the generation is slightly negative for long waves but significantly positive for short waves. The wave length dependency is probably the result of the cloud patterns associated with surface cyclones and anticyclones imbedded in the 500 mb flow. It is postulated that the cloud patterns also cause a positive generation due to diabatic heating by solar radiation and the release of latent heat. Within a growing disturbance these diabatic effects may be an important source of energy.

1. Introduction

The earth's atmosphere may be thought of as a complex thermodynamic engine with the sun as its primary source of energy. If one assumes that as a whole the atmosphere is neither warming nor cooling, it follows that it must radiate to space the same amount of energy that it gains from the sun. However, many complicated energy transformations and interactions occur within the atmosphere and at its lower boundary before the energy is irreversibly returned to space. Because of the variable nature of the interactions which occur within the atmosphere, the amount of long wave radiation which is returned to space may show significant areal variations. The advent of the artificial earth satellite has given the meteorologist a tool with which to measure such variations. In this paper, TIROS II satellite radiation data are used in an attempt to determine the role of long wave radiation in the generation of the eddy available potential energy of the atmosphere.

The concepts of available potential energy, which were first discussed by Margules (1903), have recently been further developed by Lorenz (1955). Lorenz has defined the available potential energy as that part of the total potential energy which is available for conversion to kinetic energy. Available potential energy, which may be partitioned into zonal and eddy portions, is created by the differential heating or cooling of the atmosphere. The

zonal portion is determined by the strength of the north-south variance of zonal mean temperature distribution and is produced by a latitudinal covariance of the zonal means of diabatic heating and temperature. The eddy portion is a measure of the east-west thermal variance and is produced either indirectly by the action of eddies on the zonal available potential energy or directly by an east-west covariance of diabatic heating and temperature. Within the atmosphere the diabatic heating represents the combined effects of solar and terrestrial radiation, latent heat of condensation, and eddy conduction.

An energy balance study by Clapp (1961) of the heat sources and sinks in the lower troposphere indicated that a positive generation of eddy available energy by diabatic processes occurs at the scale of climatological long waves. On the other hand, Wiin-Nielsen and Brown (1962) and Winston and Krueger (1961) found that at the eddy scale diabatic processes tend to destroy available potential energy.

In this paper the role that one of the diabatic processes -- terrestrial radiation -- plays in the production of eddy available potential energy is considered. In particular, the importance of differences in outgoing long wave radiation between various portions of a composite 500 mb wave pattern is studied. Although these differences represent differential cooling

rather than heating of the atmosphere, their effect on the production of eddy available potential energy is the same. The difference in outgoing long wave radiation above surface cyclones and anticyclones and its possible consequence is also briefly considered.

2. Data and Procedures

The basic data employed consisted of infrared radiation measurements made by TIROS II and of 500 mb and surface synoptic charts. The TIROS II data were obtained for 27 days between November 26, 1960 and January 7, 1961. For each of these days the Meteorological Satellite Laboratory of the United States Weather Bureau prepared daily composite radiation maps for channel four of the five-channel scanning radiometer aboard TIROS II. The channel four radiometer measured radiation in the 7.2 - 32.6 micron band. With the corrections that were made for the nonflatness response of the filters, the channel four data essentially represent the total radiation emitted from the earth-atmosphere system. The radiation maps, printed on a mercator projection with a 1:20,000,000 scale, covered most of the area between 50°N and 50°S. Only radiation values which were obtained by averaging ten or more discrete readings from the Final Meteorological Radiation Tape were used. These values, which represent measurements made at nadir angles of less than 56°, tend to be more reliable since they were subjected to only

minor limb darkening (Wark et. al. 1962). Details of the calibration and operation of the five-channel scanning radiometer are contained in TIROS II Radiation Data User's Manual (1961).

Synoptic data corresponding to the dates noted above were obtained from the National Weather Analysis Center 12-hourly Northern Hemisphere 500 mb and surface charts. The geographical area used in this study was limited by the availability of both radiation and synoptic weather data to an area extending from Western Europe westward across the Atlantic, North America and the Pacific to Japan between latitudes 30^{o}N and 50^{o}N.

Estimates of the generation of eddy available potential energy due to long wave radiation were made by using the above data to calculate the covariance between the radiation and thickness fields associated with 500 mb waves. The computations were based on **Lorenz'** (1955) expression for the generation of eddy available potential energy,

$$G_e = g^{-1} \int_0^{\bar{P}_o} \frac{\Gamma_d}{(\Gamma_d - \bar{\Gamma})\bar{T}} \left(\overline{T^* Q^*}\right) dp \qquad (1)$$

where g is the acceleration of gravity, $\bar{P}_o$ is the average surface pressure, Γ_d is the dry adiabatic lapse rate, $\bar{\Gamma}$ is the mean lapse rate on a constant pressure surface, $\bar{T}$ is the mean temperature of the layer, and T* and Q* are the respective

deviations from their zonal averages of temperature and of the rate of addition of heat per unit mass. The expression $\overline{(T^*Q^*)}$ represents the areal mean of the covariance of temperature and heating for latitude circles. Positive generation of eddy available potential energy occurs when air warmer than the average for its latitude is warmed or air **cooler** than the average for its latitude is cooled. Although Lorenz' development of the available potential energy involves the entire mass of the atmosphere, the expression can be used to estimate the contribution from a limited portion of the atmosphere.

As noted earlier, Q* represents the combined effects of the differential heating due to solar radiation, infrared radiation, latent heat of condensation, and heating by eddy conduction. In this study only the contribution of the infrared radiation is considered. Thus Q* has been replaced by the deviations of the divergence of infrared radiation from its latitudinal mean; that is,

$$Q^* = g\left(\frac{\partial R}{\partial p}\right)^* \qquad (2)$$

where R represents the net infrared radiation. The deviations of the 1000-500 mb thickness from its latitudinal mean were used as a measure of T*. Substituting (2) into (1) and using the hydrostatic relationship to replace temperature by thickness gives for the 1000-500 mb layer

$$G_e = \int_{500\,mb}^{1000\,mb} \frac{\Gamma_d}{(\Gamma_d - \bar{\Gamma})\,\bar{h}} \left[\overline{h^* \left(\frac{\partial R}{\partial p}\right)^*}\right] dp \qquad (3)$$

where h* is the deviation of the 1000-500 mb thickness from $\bar{h}$, the mean thickness for the area of the wave. Since the mean latitude at the area covered by the wave is 40°N, $\bar{h}$ essentially represents a latitudinal mean based on data obtained from the longitudinal sectors mentioned previously. The values used for the constants were $\Gamma_d = 9.8^{\circ}C\ km^{-1}$, $\bar{\Gamma} = 6.5^{\circ}C\ km^{-1}$, and $\bar{h} = 17{,}830$ feet (calculated from the data). Substituting these values into (3) and approximating the integral gives

$$G_e = -1.66 \times 10^{-4} \left(\overline{h^* R^*}\right) \qquad (4)$$

where R* now represents the deviations of the TIROS II infrared measurements from their latitudinal mean. This computational form of the equation was used to obtain an estimate of the eddy generation in 1000-500 mb layer.

The evaluation of the covariance term $(\overline{h^*R^*})$ is based on certain assumptions. First, it must be assumed that satellite measurements provide reasonable estimates of the divergence of radiation within the column of air beneath the satellite. Using observations made from balloon-borne radiometers, Sabatini and Suomi (1961) found a correlation

of 0.88 between observation of outgoing radiation at the top of the soundings (about 34 mb) and the divergence of radiation within the column of air beneath. Since it is likely that the outgoing radiation at 34 mb is not much different from that at the top of the atmosphere, the satellite observation should provide reasonable estimates from which R* may be calculated. The assumption is further supported by the initial results obtained by Smith (1964) who has correlated the divergence of radiation (measured by radiometersondes) within various layers of the atmosphere with satellite measurements of infrared radiation over the same area. The correlations he achieved increased as he used thicker layers; however, only small increases were noted for layers thicker than the 1000-600 mb layer. Thus it appears that a reasonable, although not ideal, estimate of the $\overline{(h^*R^*)}$ may be obtained by calculating the covariance between satellite measurements of the infrared flux and the 1000-500 mb thickness.

Principal attention was given to the generation of eddy available potential energy due to variations in radiational cooling between various portions of a composite 500 mb wave. Individual 500 mb wave patterns were analyzed by drawing ridge lines, trough lines, and inflection lines through those waves which covered a latitudinal span of at

least ten degrees within the zone between 30° N and 50° N. The inflection lines, which were constructed by connecting inflection points on successive contours, were drawn both ahead and behind troughs (or ridges). As expected most lines were oriented generally north-south. The 500 mb heights were then read along each trough, ridge, and inflection line at one degree intervals of latitude. The 1000-500 mb thickness was also calculated for each point, and from these calculations h^* was computed.

The lines were then transposed to the radiation maps and radiation values read at each interval. When the time of the radiation measurements did not coincide with the synoptic map time, the positions of the lines were interpolated between two maps. Because of the lack of data some lines had only a few radiation data points. Only those lines which had at least three points were used. The values of R^* were approximated by taking the deviations of the radiation values from the latitudinal means calculated by Astling and Horn (1964), who used the same TIROS II data that has been used here. The values R^* and h^* were then used to evaluate equation (4) to obtain an estimate of the eddy generation within the 1000-500 mb layer.

Because of the incompleteness of the satellite radiation data, it was not possible to obtain good measurements of the role of atmospheric infrared radiation in generating

eddy available potential energy within individual waves. Therefore, the radiation and thickness data from a number of individual situations were combined to form the basis of a model of a composite 500 mb wave. Means for each of the parameters (latitude, radiation and thickness) were computed separately for each portion of the wave (i.e. for trough line, ridge line and inflection lines). Since the mean latitude of each line was within one degree of 40°N the results in effect represent the variation of these quantities through a composite 500 mb wave at 40°N.

A less extensive study was made of the differences in radiational cooling above surface cyclone and anticyclone centers. The centers were plotted on radiation maps, interpolations being made when the map times differed from the times of the satellite measurements. The radiation value for each center was determined by taking a mean of the values printed on the radiation map within two and one half degrees of longitudes east and west of the surface center. Because of the considerable north-south variation in radiation, values north and south of the center were not used. Sixteen cyclone and twenty-five anticyclone centers were found for which adequate satellite data were available.

3. Results

A. Surface Cyclones and Anticyclones. Before examining the generation of eddy available potential energy within disturbances which appear at 500 mb, let us briefly examine the differences in outgoing radiation which occur between

surface cyclones and anticyclones.

The infrared radiation values associated with cyclone and anticyclone centers are presented in Table 1. The mean radiation value calculated for sixteen surface cyclones with a mean latitude of 42.3° N was 264 mly min^{-1}. Interpolating between the latitudinal means computed at 40° N and 45° N by Astling and Horn (1964), a mean radiation value of 284 mly min^{-1} is obtained for 42.3° N. Thus the mean value of infrared radiation above surface cyclones was 20 mly min^{-1} lower than the latitudinal mean. On the other hand, the latitudinal mean for twenty-five anticyclone centers with a mean latitude of 39.0°N was 304 mly min^{-1} or 13 mly min^{-1} higher than the latitudinal mean of 291 mly min^{-1} obtained from Astling and Horn's data. The "Student t" test (Panofsky and Brier, 1958) was used to determine the significance of these differences. Since the mean value for cyclones was 20 mly min^{-1} lower than the mean at 42.3° N and the mean for anticyclones was 13 mly min^{-1} higher than the mean at 39°N, a difference of 33 mly min^{-1} was used in the test. This difference is significant at the 99 percent confidence level.

A study by Weinstein (1961), who used EXPLORER VII radiation data, also revealed pronounced radiation differences on a synoptic scale. Radiation values were read from Weinstein's maps for thirteen surface cyclones and eleven anticyclones. The mean value for the cyclones was 30 mly min^{-1}

less than for the anticyclones. This value compares favorably with the 40 mly min^{-1} difference found in this study.

This systematic variation of outgoing radiation with synoptic weather patterns was expected. Higher radiation values are associated with the relatively cloudless areas of anticyclones while lower values are associated with the cloudy areas of cyclones. However, these differences may or may not be significant in the generation of eddy available potential energy. To treat these differences as significant sources for the generation of eddy available potential energy, it would be necessary to assume that surface cyclones are associated with columns of air possessing a relatively high mean virtual temperature and anticyclones with relatively low mean virtual temperature. Although this may be the case, the complex structure of the atmosphere above surface systems makes it difficult to put a great deal of confidence in conclusions based on such an assumption. Consequently, a more extensive study was made of atmospheric disturbances at 500 mb.

B. 500 mb Wave Patterns. The manner in which the synoptic features at 500 mb were related to the radiation field has been outlined under "Data and Procedures". The number of data points used are listed in Table 2. The means of the various parameters, which are summarized in Table 3, represent conditions associated with a composite 500 mb wave located at about 40°N.

The lowest mean value of outgoing long wave radiation (280 mly min^{-1}) is observed along the inflection line to the

east of the trough, while the highest mean value (300 mly min^{-1}) occurs along the inflection line to the west of the trough. The deviations of these values from the latitudinal means obtained by Astling and Horn (1964) are shown in column 3 of Table 3. The "Student t" test indicates that the difference between the radiation means at the two inflection lines is significant at the 95 percent confidence level. Again these differences were anticipated. The low value to the east of the trough can be attributed to the positive vertical motion and resulting cloudiness in that area. On the other hand, the relatively high value to the west of the trough is undoubtedly the result of sinking air and relatively clear skies.

Equation (4) was used to obtain a measure of the production of eddy available potential energy due to these synoptic scale variations of infrared radiation. The results presented in the right hand column of Table 3 indicate a small positive generation along both inflection lines, practically no generation along the trough line and a very slight negative generation along the ridge line. Assuming that the inflection lines and trough and ridge lines are equally spaced, the mean generation within the composite 500 mb wave is +0.055 watts m^{-2}. Since the data used were from only limited areas the generation value obtained represents only a contribution to the global mean generation.

Previous investigations of the eddy generation have produced a wide range of results. Suomi and Shen (1963),

using thirteen selected days of **EXPLORER VII** data, obtained a generation of +0.580 watts m^{-2} due to infrared cooling which is considerably larger than that obtained here. Other investigators have used indirect methods to estimate the generation due to the combined diabatic processes. Clapp (1961), using a heat balance approach, estimated that in the latitudinal band 30-60°N during December-February the eddy generation was +0.382 watts m^{-2}. On the other hand, Wiin-Nielsen and Brown (1962) computed a negative generation of -3.5 watts m^{-2} for latitudes 20-90°N for January 1959. Winston and Krueger (1961) also obtained a negative generation (averaging about -3.0 watts m^{-2}) for the same area for the period December 27, 1959 - January 13, 1960; however, their results revealed a marked daily variation (varying from +0.5 to -6.2 watts m^{-2}).

Using Fourier methods, Wiin-Nielsen and Brown partitioned the eddy generation according to wave number. Although they obtained a negative generation at all wave numbers (n=1-10), they found that the generation became less negative as the wave number increased. They obtained standard deviations which indicated, especially at higher wave numbers, that positive generation occurred in many cases.

To test whether a similar trend was present in the data used in this study, the 500 mb wave pattern data were partitioned according to wave length. The length of each 500 mb wave was estimated by counting the number of degrees of

longitude between the trough and ridge lines and multiplying this value by two. For convenience of discussion the various wave lengths (in degrees longitude) were divided into 360^{o} to obtain their wave number equivalents (n). The eddy generation was then computed for three groups of wave numbers ($n > 9$, $n = 6\text{-}9$, and $n < 6$). The results for the three groups, which are presented in Table 4, indicate a small negative generation (-0.074 watts m^{-2}) for the longest waves ($n < 6$); a small positive generation (+0.063 watts m^{-2}) for the intermediate waves ($n = 6\text{-}9$); and a considerably larger positive generation (+0.193 watts m^{-2}) for the short waves ($n > 9$). This trend agrees with that noted by Wiin-Nielsen and Brown (1962). However, in comparing these results it is important to remember that the results reported here involve only the effect of terrestrial radiation while the work of Wiin-Nielsen and Brown included the combined effect of all diabatic processes.

Although no calculation of the other diabatic terms was attempted here, it appears likely that at short wave lengths two of the terms provide additional eddy generation while one acts negatively. The direct absorption of solar radiation should be largest where thick clouds are present; that is, in the region to the east of the trough. Theoretical computations by Korb and Möller (1962) indicate that the direct absorption of solar radiation in the cloudy, moist air to the east of a trough may be twice as great as in the clear, dry air to the west of a trough. The greater

absorption thus occurs in the portion of the 500 mb wave which is already warmer than the mean and thus produces eddy available potential energy. Likewise, the release of latent heat of condensation which is largest in the cloudy area in advance of the trough, should contribute positively to the generation. Clapp and Winninghoff (1963), have computed values of solar radiation absorption and latent heat release in the 1000 - 200 mb layer which agrees favorably with the concepts presented here. The remaining diabatic term --sensible heating due to eddy conduction-- obviously destroys eddy available potential energy. As cold air flows southward it is warmed through eddy conduction, while to a lesser extent warm air which flows northward is cooled. This effect is especially large over the western portions of high and middle latitude oceans during the winter season when continental polar air flows over the sea.

Although the overall eddy generation by infrared radiation calculated here (+ 0.055 watts m^{-2}) is quite small, the results indicate that the generation is very dependent on the scale of the eddies. At long wave lengths the combined diabatic processes are no doubt quite effective in destroying eddy available potential energy. However, at short wave lengths ($n > 9$) the generation by infrared radiation is appreciable (+0.193 watts m^{-2}), and it is likely that at those wave lengths the direct absorption of solar radiation and release of latent heat also contribute significantly to the positive generation. The long waves, which

are often viewed as climatological in nature, tend to be produced by topography and ocean-continent distribution of the earth and thus frequently lack the distinct cloud and weather patterns which are associated with shorter travelling waves. It is within these transient waves that significant positive generation may occur.

It seems quite possible that the generation at the short wave scale plays an important role in the growth of disturbances. For example, a weak disturbance (i.e., a short wave of small amplitude) with the "right" distribution of clouds may generate within itself a significant amount of eddy available potential energy. The occurrence of weak disturbance which produce distinct cloud and precipitation patterns as they move across the United States is not unusual. Because the disturbance is weak, it will not have yet produced a strong southward flow of cold air (or northward flow of warm air). Consequently, the negative effect produced by sensible heating will be small compared with the positive generation by infrared and solar radiation and release of latent heat. This weak disturbance may then grow as it feeds on these sources of eddy available potential energy. As the wave amplifies it will disturb the zonal temperature field causing a conversion of zonal available potential energy to eddy available potential energy. This new source of eddy energy may then become the dominant one, causing a major development. Thus it appears that the direct generation of eddy available potential energy

by diabatic processes may be of considerable importance in the early stages of certain developing disturbances. Although the direct generation is not the main source of energy, it may frequently act as a trigger in the growth of a storm. Any quantitative discussion of this possibility is beyond the scope of this paper; however, the results obtained here indicate that studies of individual cases should be undertaken.

4. Summary and Conclusions

The TIROS II measurements reveal that definite infrared radiation patterns occur on a synoptic scale. Over surface cyclones the outgoing radiation is significantly less than the mean for the latitude, while over surface anticyclones it exceeds the mean for the latitude. These differences are undoubtedly due to the distribution of cloudiness, especially middle and high level cloudiness.

A study of the infrared radiation patterns associated with a composite 500 mb wave show relatively high values to the west of the trough and relatively low values to the east. A calculation of the covariance of the radiation values and 1000-500 mb thickness reveals that these radiation differences tend to generate eddy available potential energy. When the data are partitioned according to the length of the 500 mb waves, a distinct variation of the generation is noted. At long wave lengths ($n < 6$) the infrared radiation tends to destroy eddy available potential energy. At intermediate

wave lengths (n = 6-9) there is a small positive generation and at short wave lengths (n > 9) there is a larger positive generation. This dependence on wave length appears to be due to the patterns of cloudiness associated with the various waves. The longer waves do not have as distinct a distribution of clouds as do the shorter waves.

Because of the cloud patterns associated with the shorter waves, the diabatic heating due to direct absorption of solar radiation and release of latent heat may also contribute to the generation of eddy available potential energy. In both cases the greatest heating tends to occur in the portion of the wave which is already warmer than the mean for the latitude. The remaining diabatic term -- sensible heating by eddy conduction -- destroys eddy available potential energy. In a wave of small amplitude the diabatic effects of infrared and solar radiation and latent heat probably exceed the effect of sensible heating and thus cause a significant generation. This supply of eddy available potential energy may be important during the early stages of a growing disturbance.

In general the results indicate that increasing attention should be given to the scale of atmospheric energy processes. A simple partition of a quantity such as available potential energy into zonal and eddy portions seems inadequate.

5. Acknowledgements

The authors wish to thank Mr. Donald Johnson, Mr. Elford Astling, Mr. Phillip Smith, Mr. Alfred Carasso and Mr. William Smith for their help in various stages of this study. This research has been supported by Project 4 of U. S. Weather Bureau Grant 10.

TABLE 1

Radiation Values For Surface Cyclones and Anticyclones

Cyclones

Location	Central Pressure (mb)	Greenwich Date	Approximate Time of Observation (Greenwich)	Radiation (Mly/Min)
44N 011E	1008	28 Nov 60	0900	210
45N 020E	1006	29 Nov 60	0800	270
48N 023E	1002	12 Dec 60	0300	240
37N 128W	1003	14 Dec 60	1300	240
40N 002E	998	14 Dec 60	0500	230
48N 088W	994	15 Dec 60	0700	270
31N 079W	1006	16 Dec 60	0300	330
37N 003E	1003	16 Dec 60	0500	220
39N 177E	994	17 Dec 60	1000	320
37N 001W	1006	17 Dec 60	0500	290
48N 146W	994	18 Dec 60	1000	300
42N 008E	1006	18 Dec 60	0200	280
50N 158W	968	21 Dec 60	1100	300
48N 158W	964	25 Dec 60	0800	250
46N 033E	995	28 Dec 60	2100	220
37N 028E	1009	31 Dec 60	2100	250

Mean Latitude 42.3° N

Mean Radiation 264 mly/min

Standard Deviation 35 mly/min

Anticyclones

40N 020W	1033	28 Nov 60	1300	240
38N 167W	1035	29 Nov 60	1600	330
39N 014W	1031	29 Nov 60	1200	360
44N 001E	1031	29 Nov 60	1000	310
34N 039E	1025	29 Nov 60	1000	350
41N 109W	1033	14 Dec 60	0600	280
40N 030W	1033	14 Dec 60	1200	320
39N 027W	1034	15 Dec 60	0600	270
45N 047W	1038	17 Dec 60	0700	320
45N 025W	1032	21 Dec 60	0400	340
46N 020W	1031	22 Dec 60	0300	290
31N 087W	1035	23 Dec 60	0900	320
45N 037W	1044	23 Dec 60	0400	300
42N 037W	1032	27 Dec 60	0200	320
35N 127E	1030	2 Jan 61	0700	310
42N 132W	1030	2 Jan 61	0100	290
42N 117W	1029	2 Jan 61	0100	250
36N 025W	1032	2 Jan 61	0100	320
34N 018W	1033	3 Jan 61	0000	280
36N 178E	1029	5 Jan 61	0200	260
42N 113W	1031	5 Jan 61	0400	310
32N 090W	1031	5 Jan 61	0400	330
33N 030W	1030	4 Jan 61	0000	300
42N 111W	1036	6 Jan 61	0000	280
31N 158W	1022	7 Jan 61	0000	320

Mean Latitude 39.0° N

Mean Radiation 304 mly/min

Standard Deviation 29 mly/min

TABLE 2

500 mb Feature	Mean Latitude	No. of cases (i.e., lines)	Total Data Points	Data Points Per Case
Trough	40.2°N	60	567	9.4
Ridge	40.4°	63	551	8.7
Inflection East	40.8°	40	304	7.6
Inflection West	40.4°	34	331	9.7
Total		197	1753	8.9

Inflection East is inflection line east of trough
Inflection West is inflection line west of trough

TABLE 3

500 mb Feature	R	$\sigma(R)$	R^*	h	$\sigma(h)$	h^*	G_e
Trough	290	43	+1	17630	482	-250	+.029
Ridge	297	37	+8	18040	385	+160	-.148
Inflection East	280	42	-9	18070	406	+190	+.198
Inflection West	300	35	+11	17770	446	-110	+.140
Means	289**			17880			+.055

R : Satellite Radiation Value (mly/min)

$\sigma(R)$: Standard Deviation of Radiation Values (mly/min)

R^*: Deviation of Radiation Value from Mean (mly/min)

h : 1000 - 500 mb Thickness (feet)

$\sigma(h)$: Standard Deviation of Thickness Values (feet)

h^*: Deviation of Thickness from Mean (feet)

G_e: Generation of Eddy Available Potential Energy (watts/m^2)

** Mean value of radiation is for 40°N from Astling and Horn (1964)

TABLE 4

500 mb Feature	N	Lat.	R	$\sigma(R)$	R^*	h	$\sigma(h)$	h^*	G_e
Short Waves (n > 9)									
Trough	151	40.7°N	291	36	+2	17860	324	-20	+.005
Ridge	204	40.9	293	35	+4	17960	328	+80	-.037
Inflection East	46	39.8	268	31	-21	18210	365	+330	+.805
Inflection West	60	39.8	289	43	0	17750	372	-130	0
							Net Generation		+.193
Medium Waves (n = 6-9)									
Trough	219	40.1	296	53	+7	17590	508	-290	+.235
Ridge	176	40.6	295	42	+6	18030	438	+150	-.105
Inflection East	136	41.0	288	46	-1	18020	388	+140	+.016
Inflection West	185	39.8	304	35	+15	17820	434	- 60	+.105
							Net Generation		+.063
Long Waves (n < 6)									
Trough	197	39.9	281	31	-8	17500	489	-380	-.352
Ridge	171	39.5	303	34	+14	18150	360	+270	-.438
Inflection East	122	40.9	276	39	-13	18070	426	+190	+.286
Inflection West	86	42.1	298	27	+9	17680	499	-200	+.209
							Net Generation		-.074

N : Number of Data Points

Lat: Latitude (°N)

R : Satellite Radiation Value (mly/min)

$\sigma(R)$: Standard Deviation of Radiation Values (mly/min)

R^* : Deviation of Radiation Value from Mean (mly/min)

h : 1000 - 500 mb Thickness (feet)

$\sigma(h)$: Standard Deviation of Thickness Values (feet)

h^* : Deviation of Thickness from Mean (feet)

G_e : Generation of Eddy Available Potential Energy (watts/m^2)

Inflection East is inflection line East of Trough

Inflection West is inflection line West of Trough

References

Astling, E. G. and L. H. Horn, 1964: Some Geographical Variations of Terrestrial Radiation Measured By TIROS II, Journal of the Atmospheric Sciences, Vol. 21, No. 1.

Clapp, P. F., 1961: Normal Heat Sources and Sinks in the Lower Troposphere in Winter, Monthly Weather Review, Vol. 89, No. 5.

Clapp, P. F. and F. J. Winninghoff, 1963: Tropospheric Heat Sources and Sinks at Washington, D. C., Summer 1961, Related to the Physical Features and Energy Budget of the Circulation, Monthly Weather Review, Vol. 91, No. 10.

Korb, G. and F. Möller, 1962: Theoretical Investigation of Energy Gain by Absorption of Solar Radiation in Clouds, Ludwig-Maximilians Universität, Meteorologisches Institut, München, Germany, Contract DA-91-591-EUC-1612.

Lorenz, E. N., 1955: Available Potential Energy and the Maintenance of the General Circulation, Tellus, Vol. 7, No. 2.

Margules, M., 1903: Uber Die Energie der Sturme, Translated in Smithsonian Miscellaneous Collections, 51, 1910.

Panofsky, H. A. and G. W. Brier, 1958: Some Applications of Statistics to Meteorology, Pennsylvania State University, University Park, pp. 58-64.

Sabatini, R. R. and V. E. Suomi, 1962: On the Possibility of Atmospheric Infrared Cooling Estimates From Satellite Observations, Journal of the Atmospheric Sciences, Vol. 19, No. 4.

Smith, William L. (1964): Personal Communication.

Suomi, V. E. and W. C. Shen, 1963: Horizontal Variation of Infrared Cooling and the Generation of Eddy Available Potential Energy, Journal of the Atmospheric Sciences, Vol. 20, No. 1

TIROS II Radiation Data User's Manual, 1961: NASA, Goddard Space Flight Center, Green Belt, Maryland, May 15.

Supplement TIROS II Radiation Data User's Manual, 1962: NASA, Goddard Space Flight Center, Green Belt, Maryland, May 15.

Wark, D. Q., G. Yamamoto and J. H. Lienesch, 1962: Methods of Estimating Infrared Flux and Surface Temperature from Meteorological Satellites, Journal of the Atmospheric Sciences, Vol. 19, No. 5.

Weinstein, M., and V. E. Suomi, 1961: Analysis of Satellite Infrared Radiation Measurements on a Synoptic Scale, Monthly Weather Review, Vol. 89, No. 11.

Wiin-Nielsen, A. and J. A. Brown, 1962: On Diagnostic Computations of Atmospheric Heat Sources and Sinks and the Generation of Available Potential Energy, Proceedings of the International Symposium on Numerical Weather Prediction in Tokyo, pp. 593-613.

Winston, J. S. and A. F. Krueger, 1961: Some Aspects of a Cycle of Available Potential Energy, Monthly Weather Review, Vol. 89, pp. 307-318.